Ewart, T.E. and S.A. Reynolds, Acoustic implications of a new model, Proceeding of the 'Aha Huliko'a 1991 Hawaiian Winter Workshop, 399-416, 1992.

ACOUSTIC IMPLICATIONS OF A NEW MODEL

Terry Ewart and Stephen Reynolds
Applied Physics Laboratory
University of Washington
Mailstop HN 10
Seattle, Wa. 98115

ABSTRACT

We attempt to show that the use of stochastic inverse methods allows us to precisely test proposed models of oceanic dynamical structure. It is the integrative property of the propagating acoustic wave that enables us to "view" ocean dynamics on scales that would be impossible with traditional ocean instrumentation. Unfortunately, because there has been a lack of propagation experiments conducted where the ocean dynamics are well understood, we are unable to fully demonstrate the use of the concepts we present. Additional investigations are required. Theoretical and numerical studies of acoustics in "numerical oceans" can provide new information on the scales of ocean dynamics that are important for sound propagation. In turn, this information will tell us how thoroughly we need to model ocean variability in order to predict propagation characteristics. We show that the important scales of ocean variance are much larger than the acoustic wavelength, when the ranges correspond to standard range/frequency combinations. Finally, we present some ideas for future work using acoustics to verify a "new model," and discuss the temporal and spatial scales for a possible experiment.

INTRODUCTION

Our comprehension of wave propagation in random media has progressed to the point where theoretical predictions of the fluctuations in sound waves that have passed through a medium with a known autocorrelation function of the acoustic index of refraction are quite accurate. Thus, the focus of the 'Aha Huliko'a meeting on "new" ocean dynamical and internal wave models is not only an important step in improving our understanding of ocean processes, but could herald a significant advance in our ability to test acoustic scattering predictions. In this paper, we have attempted to provide an overview of the elements of ocean dynamics required by the acoustician to make the ocean/acoustics link.

First, we present a brief review of the parameterization of ocean internal waves and finestructure

Applied Physics Laboratory
College of Ocean and Fishery Sciences, University of Washington

1943–1993 — 50 Years of Excellence

February 14, 1994

The final technical reports are being sent to you in conformance with ONR report distribution requirements, contract N00014-92-J-1647.

Enclosed: 2 reports

1013 NE 40th Street Seattle, Washington 98105-6698 (206) 543-1300 FAX (206) 543-6785

used in acoustic propagation theory, and illustrate some of the progress being made in predicting acoustic scattering. Second, using a specific example, we demonstrate the power of ocean acoustic stochastic inverse methods. Note that, by stochastic inverse, we mean "imaging" the correlation or spectral properties of the index of refraction field rather than the index of refraction itself. We then discuss how one sets limits to the wavenumber/frequency bandwidth requirements of ocean models in the context of acoustic scattering. Finally, we present some ideas for a future coordinated ocean/acoustics research effort.

Ocean internal waves have a dramatic effect on sound propagation. Consider the numerical examples of acoustic propagation shown in Figure 1. The intensity of a sound wave propagating in the depth/range plane is shown for depths to 4000 m and for the range interval from 35 to 65 km. Figure 1(a) has a vertical sound speed profile that is range-independent. Figure 1(b), in addition to the range-independent profile of 1(a), includes random internal wave induced fluctuations. Sharp foci of sound channel convergences are seen in 1(a). In 1(b), the internal wave perturbations have destroyed the foci and the sound field has broken up into ribbons of intensity. These ribbons of sound have been directly observed and are discussed in a paper by Uscinski and Potter (1988). We wish to predict the scattering statistics of these wave fields, and exploit them using stochastic inverse methods. In a discussion of internal waves, two points regarding acoustic propagation must be emphasized: (1) Because sound is the only form of energy (other than neutrinos) that can propagate long distances in the sea, it may be possible to monitor the ocean using inversion of information on acoustic travel time. (2) In order to study sound propagation in the stochastic ocean, the dynamical space/time statistics must be known.

SOUND VELOCITY FLUCTUATIONS IN A STOCHASTIC OCEAN

The coordinate system we use to discuss stochastic ocean behavior is shown in Figure 2. The two-point separation coordinates are $\xi = x_1 - x_2$, $\eta = y_1 - y_2$, $\zeta = z_1 - z_2$, $\tau = t_1 - t_2$, and the Fourier conjugate variables in the wavenumber/frequency domain are α_1, α_2, β, and ω. Propagation takes place in the x-direction.

Following Uscinski (1986), the index of refraction, n, is written as the sum of a depth-dependent deterministic component, n_d, and a stochastic component, n_1.

$$n(x, y, z, t) = 1 + n_d(z) + \langle\mu^2\rangle^{1/2} n_1(x, y, z, t). \tag{1}$$

The rms index of refraction fluctuation, $\langle\mu^2\rangle^{1/2}$ is related to sound speed fluctuations, δC (arising from vertical displacements or velocities in the propagation direction),

$$\langle\mu^2\rangle^{1/2} = \frac{\langle\delta C^2\rangle^{1/2}}{C_o}, \tag{2}$$

where C_0 is the reference sound speed. We represent the two-point statistics of $n_1(x, y, z, t)$ by the power spectrum,

$$S(\alpha_1, \alpha_2, \beta, \omega). \tag{3}$$

In general, $\langle\mu^2\rangle$ is a function of depth. However, if a ray traverses a narrow range in depth, $\langle\mu^2\rangle$

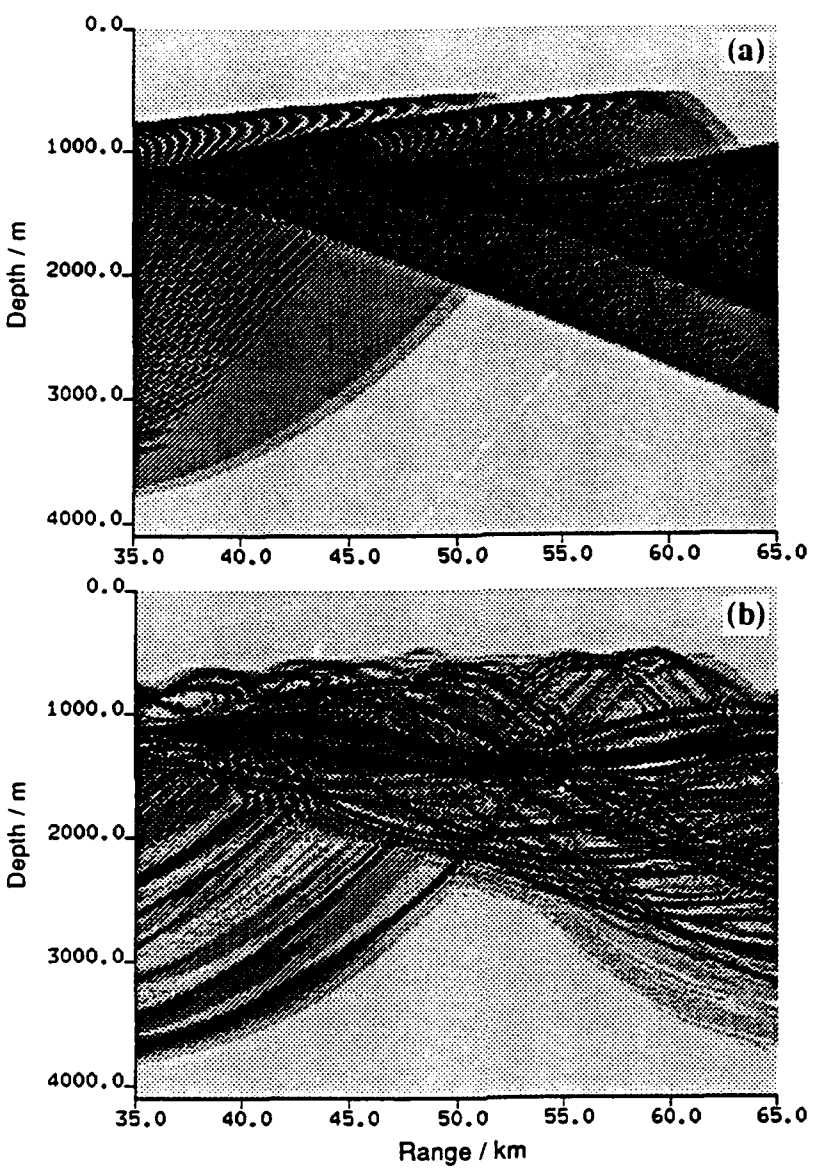

Figure 1. The intensity of a sound wave propagating in the depth/range plane is shown for depths to 4000 m and for the range interval from 35 to 65 km. The vertical sound speed is derived from the Munk canonical profile, and propagation is calculated using a wide angle parabolic equation (PE) code. The narrow beam source is above and near the axis of the sound channel. (a) Range-independent case, without internal waves. One sees sharp foci due to sound channel convergences. (b) As in (a) with internal wave variability added into the environment. The rms internal wave displacement is 7.3 m. The foci are smeared and diffuse and ribbons of intensity have formed.

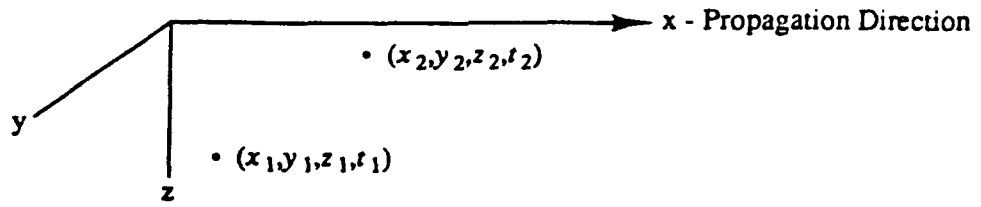

Figure 2. Coordinate system.

can be considered constant. Subsequently, we will discuss experiments carried out at Cobb Seamount in the N.E. Pacific at a depth of 1000 m, and this is such a region. For the general case, the depth dependence provides little or no difficulty for simulations but adds complexity to theoretical predictions of the moments of the acoustic field. We impose the traditional internal wave assumptions of horizontal isotropy and vertical homogeneity on the medium statistics. For simplicity, we will assume that locally the buoyancy frequency, and hence $<\mu^2>$ is depth independent. Under these conditions, the space/time spectrum of $n_1(x,z,t)$ may be written,

$$S(\alpha,\beta,\omega), \quad \text{where} \quad \alpha^2 = \alpha_1^2 + \alpha_2^2. \tag{4}$$

(We define the spectrum such that the integral over positive frequencies and wavenumbers is $\equiv 1$.) The horizontally isotropic medium correlation function is,

$$R(\xi,\eta,\zeta,\tau) = <\mu^2> \boldsymbol{F}\left\{S(\alpha,\beta,\omega)\right\}, \tag{5}$$

where $\boldsymbol{F}\{..\}$ indicates a Fourier transform. Note that $R(0,0,0,0) = <\mu^2>$. In the theoretical treatment of scattering, the medium is represented by a projection of the medium correlation function in the direction of wave propagation called the transverse correlation function (TCF). The TCF is obtained from the correlation function by

$$R_\perp(\zeta,\tau) = \int_{-\infty}^{\infty} \frac{R(\xi,\zeta,\tau)\,d\xi}{R(0,0,0)} = \int_{-\infty}^{\infty} \frac{R(\xi,\zeta,\tau)\,d\xi}{<\mu^2>}. \tag{6}$$

$R_\perp$ is the function we will discuss in the stochastic ocean context. The Fourier transform of $R_\perp$ is written $S_\perp(\beta,\omega)$, and is called the transverse spectrum. Note that η, the transverse horizontal coordinate, has been suppressed (i.e. $\eta = 0$). The η separations will not be treated here.

The ocean processes we consider are tides, internal waves and finestructure. Finestructure is the name given to the poorly understood portion of oceanic fluctuations in space and time that do not possess a wave-like dispersion relationship, but give appreciable variance in δC. As a specific example, we turn to consider the TCF used to study the acoustic propagation regime that existed during the Mid-Ocean Acoustic Transmission Experiment (MATE).

THE MATE TCF

At the 'Aha Huliko'a Meeting, our goal is to develop a "new" stochastic ocean model. The model we seek to replace is based on considerations of a spectrum of linear internal waves, and the parameters and spectral dependencies of the model were obtained by fitting the model to data sets, i.e. "data fits." Many authors have pointed out that linear internal waves alone cannot represent observations, and attempts to model the additional variance have been stymied by insufficient data in most experiments.

The Mid Ocean Acoustic Transmission Experiment (MATE) was designed to provide a detailed set of both temporal and spatial oceanographic and acoustic measurements. The MATE oceanographic setting (1000 m depth, Lat. 46°46'N., Long. 130°47'W) typifies open ocean

conditions. The exception is a strong baroclinic tide caused by the presence of several seamounts. The oceanographic measurements during MATE were sufficient to overdetermine $S(\alpha,\beta,\omega)$. Details of the data analysis for finestructure and internal waves are found in Levine and Irish (1981) and Levine et al. (1986). It was possible to obtain a model of $S(\alpha,\beta,\omega)$ for MATE based upon a fit to the various projections of S. We will now show that insight into the models can also be obtained from the MATE acoustical measurements.

The general form of the TCF is written for the case of separable vertical and time correlations as

$$R_{\perp IW,FS}(\zeta,\tau) = \int_{-\infty}^{\infty} \frac{R_{IW,FS}(\xi,\zeta,\tau)\,d\xi}{R_{IW,FS}(0,0,0)} = L_{p;IW,FS}\,\frac{\sigma_{IW,FS}(\zeta)}{\sigma_{IW,FS}(0)}\,\frac{\psi_{IW,FS}(\tau)}{\psi_{IW,FS}(0)}, \text{ where} \qquad (14)$$

$$L_{p;IW,FS} = R_{\perp IW,FS}(0,0).$$

For internal waves, following Uscinski (1980) we write

$$R_{\perp IW}(\zeta,\tau) = 2\,G_o^{-1}H_o^{-1}\int_{\omega_i}^{\omega_n}\frac{G(\omega)}{r_\omega}\left[\int_{\beta_c}^{\infty}\frac{H(\beta)}{\beta}\cos(\beta\zeta)d\beta\right]\cos(\omega,\tau)\,d\omega, \qquad (15)$$

where $G(\omega)$ and $H(\omega)$ are obtained from the model presented in Levine et al. (1986); r_ω arises from the internal wave dispersion relationship,

$$r_\omega^2 = \frac{\alpha^2}{\beta^2} = \frac{\omega^2-\omega_i^2}{\omega_n^2-\omega^2}, \text{ and}$$

$$G_o = \int_{\omega_i}^{\omega_n} G(\omega)d\omega, \quad H_o = \int_{\beta_c}^{\infty} H(\beta)\,d\beta. \qquad (16)$$

ω_i and ω_n are the inertial and buoyancy frequencies, respectively. β_c is the vertical wave number corresponding to the lowest internal wave mode. The model in this form is written as

$$G(\omega) = \frac{(\omega^2-\omega_i^2)^{1/2}}{\omega^p}, \quad H(\beta) = \frac{\beta_*}{\beta_*^2+\beta^2}, \quad \beta_* = t\,(\omega_n^2-\omega^2)^{1/2}. \qquad (17)$$

With the exception of the variable spectral slope, p, this model is the same as that of Desaubies (1976). The Desaubies and GM formulations (for GM see Munk (1981)) specify $p = 3$. Also, this model uses a continuous vertical wavenumber representation rather than the modal decomposition used by GM. The parameter, t, is the bandwidth parameter of Desaubies. Note that the ζ-τ or β-ω functions are separable. This fact simplifies both theory and numerical simulation.

For finestructure, we use a form based upon that of Levine and Irish (1981). They postulated two processes: one at low wavenumbers and low frequencies that is characterized by a slow decay compared to the inertial period, and another process that is characterized by high wavenumbers and frequencies, that is modulated by the internal wave field. The high wavenumber process has a very low variance, and thus little effect on acoustic propagation. It has been discussed by Ewart

et al. (1983), and will not be mentioned here except in relation to the acoustic phase correlations. The low frequency finestructure model has an asymptotic dependence in the spectral domain of α^{-2}, β^{-2}, and ω^{-2}. The forms of R_{FS} and $R_{\perp,FS}$ are

$$R_{FS}(\xi,\zeta,\tau) = \exp\left\{-\left[\left[\frac{\xi}{L_H}\right]^2 + \left[\frac{\zeta}{L_v}\right]^2\right]^{1/2}\right\} e^{-|\tau/\tau_0|}, \text{ and}$$

$$R_{\perp,FS}(\zeta,\tau) = L_{p;FS}\frac{\sigma_{FS}(\zeta)}{\sigma_{FS}(0)}\frac{\psi_{FS}(\tau)}{\psi_{FS}(0)} = L_{p,IW}\frac{\zeta}{L_v}K_1(\zeta/L_v)\, e^{-|\tau/\tau_0|}. \qquad (18)$$

We have taken $L_{p;FS} = 2 \cdot L_{H,IW} = L_{p,IW}$; K_1 is the K_1 Bessel function.

Armed with the specific form of the TCF, we now proceed to discuss the observed acoustic fluctuations and stochastic inverse predictions. For a more general discussion of the forward problem, see Ewart (1986).

A PHASE STOCHASTIC INVERSE

For fifteen days during the time that MATE oceanographic measurements were made, acoustic pulses having center frequencies near 2, 4, 8, and 13 kHz were transmitted along an 18.1 km path near 1000 m depth. These transmissions were made between a fixed set of co-located transmitters and fixed, spatially separated receivers (four receivers were located at the corners of a rectangle 3 m high by 235 m in a plane transverse to the propagation path; see Ewart and Reynolds (1984)). With a maximum angle of just over 3°, the path was nearly horizontal. The transmission path, and a single realization of the density field from source to receiver is shown in Figure 3. We wish to obtain the time-varying spectrum of this density field by stochastic inverse methods.

We can learn a great deal from the temporal correlations of the acoustic phase. (Aside: in a geometric scattering environment, pulse travel time and phase are interchangeable.) The tidal, internal wave and finestructure processes are clearly seen in the phase spectrum from the 15 day 2 kHz data set (Figure 4). The phase spectra for the other frequencies of MATE are virtually identical out to temporal frequencies well above the buoyancy frequency, indicating the geometric nature of the phase fluctuations. The spectrum has been expressed in $<\mu^2>$ units by multiplying the measured travel times by $C_o / (L_p R)^{1/2}$, with $C_o = 1480$ m/s, $L_p = 4600$ m, and $R = 18.1$ km. The validity of this conversion relies upon the travel time being geometric. The integral of the spectrum is $<\mu^2>$. The diurnal, semidiurnal, and quarter-diurnal (overtone of the semidiurnal) tidal lines are evident, as is the sharp drop-off at ω_i and ω_n. The dashed lines indicate a fit to the deterministic tides using a simultaneous deterministic/stochastic inverse to a model that includes a trend function, tides, finestructure and internal waves. The finestructure and internal waves were modeled as the Fourier transforms of Equations 15 and 18, respectively. (If the phase is geometric, the phase spectrum is related to the Fourier transform of the TCF; see Uscinski (1986).) The tides were modeled as a sum of sine and cosine terms with independent coefficients. This stochastic inverse method is the frequency domain equivalent to the inverse published by Ewart (1986) where the correlation function was used. The results of the inverse can be used to remove the deterministic functions from the time series. The 2 kHz acoustic phase record in the time domain is shown in Figure 5, before and after removal of the trend and tide

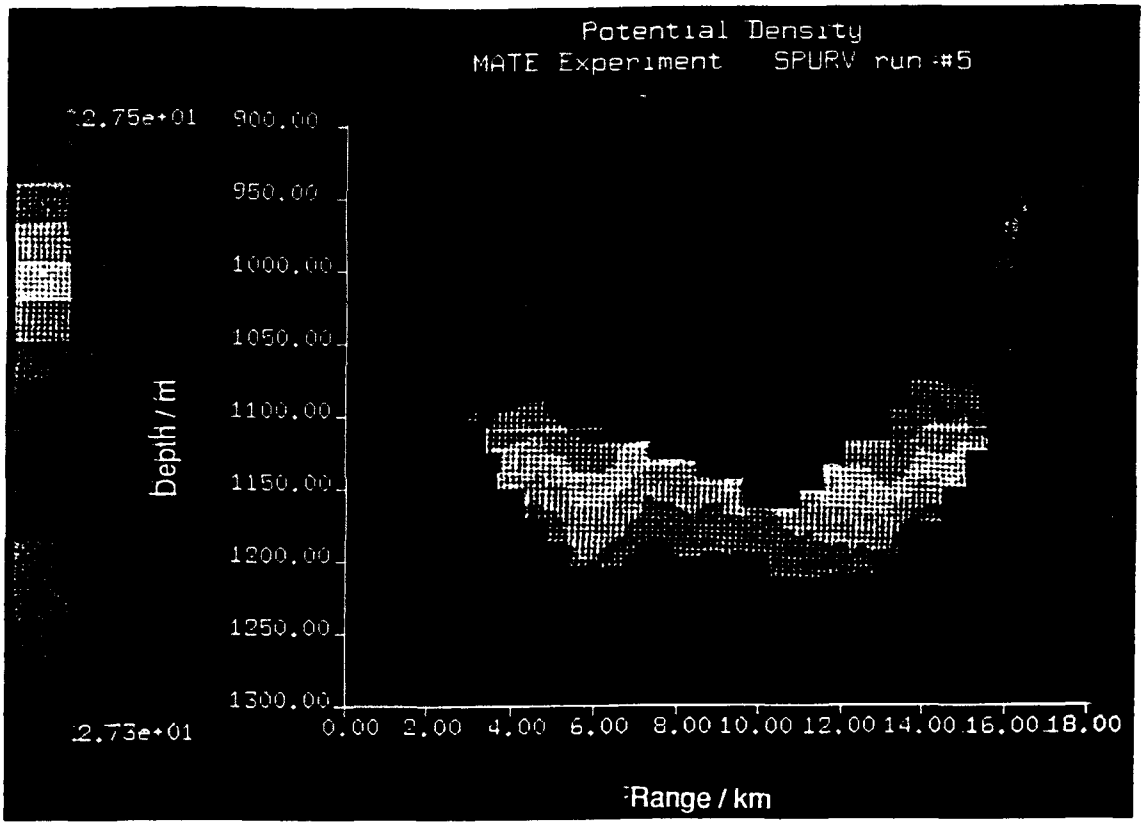

Figure 3. A single realization of the density field along the MATE transmission path from source to receiver. The measurements were obtained from a depth cycling run of SPURV. The potential density shades range from 27.3 (top) to 27.5.

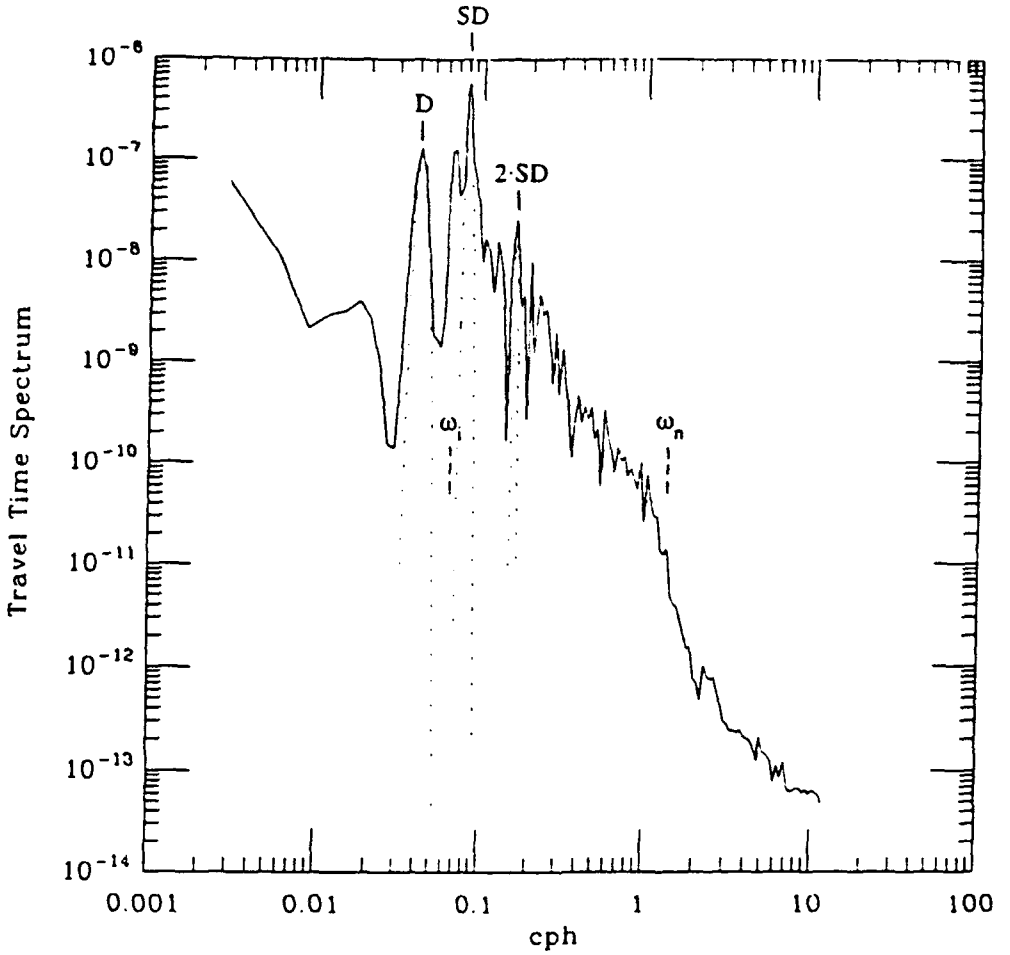

Figure 4. MATE 2 kHz travel time (phase) spectrum in $<\mu^2>$ units per cycle per hour. The spectral estimate was computed using the DPSS method described by Slepian (1978). Four discrete, prolate spheroidal windows were used. The dashed lines are the tidal components obtained by the fit described in the text; the spectral windows are evident in the tide lines.

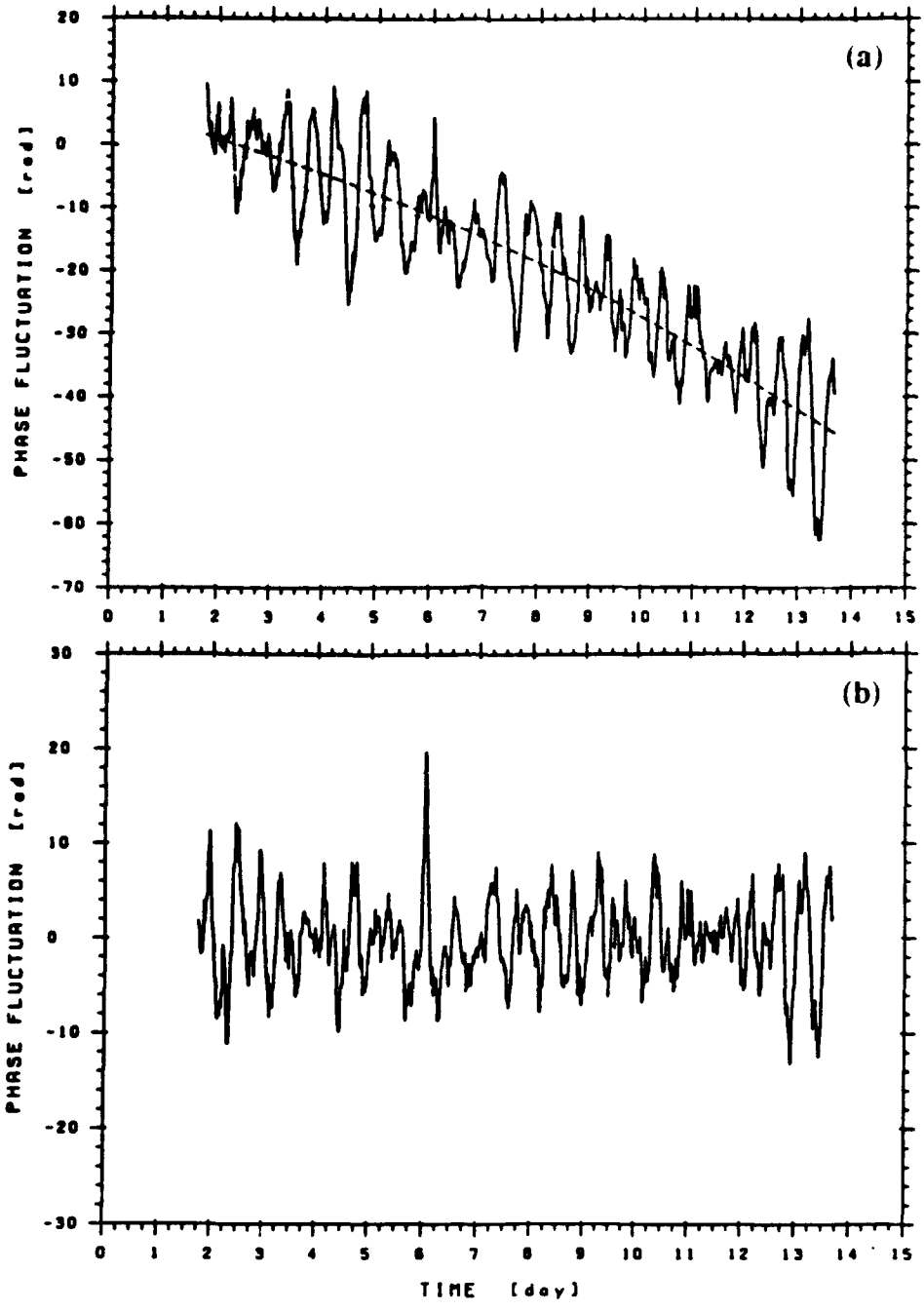

Figure 5. 2 kHz phase data in the time domain: (a) as recorded, and (b) with the deterministic trend and tidal components removed. The trend function is shown by the dashed line in (a). Note that the vertical scales are different.

model. Although the determinism of the tides is assumed, the large baroclinic tide is almost certainly time dependent over the 15 days.

To compare the travel time spectrum to the more familiar moored temperature spectrum, a similar inversion is applied to the temperature time series. The 30 day temperature record is windowed to the same 15 day period as the acoustic data and resampled to the same time grid. The modeled form of the temperature spectrum is a different integral of $S(\alpha,\beta,\omega)$, i.e., the moored spectrum:

$$\int_{-\infty}^{\infty}\int_{-\infty}^{\infty} S(\alpha,\beta,\omega)\, d\alpha\, d\beta\,. \tag{19}$$

To get the moored spectrum at the ray depth in $<\mu^2>$ units, we convert the temperature fluctuations to sound speed changes and use Eq. (2). Plots of both the travel time and temperature spectra in these units are illustrated in Figure 6. The plots include only the stochastic components, with the tidal components removed as described above.

Three distinct regions, separated by ω_i and ω_n are indicated. The modeled ω-dependence for each region is shown. Region I is represented by the low wavenumber/low frequency finestructure given by Eq. (18). We see that the moored and the travel time spectra are identical within statistical limits. These limits are large due to the short (15 day) time record. This supports the model having no distinct dispersion relation (i.e. the moored temperature spectrum and the travel time spectra have the same spectral slope). The 500 hour value of τ_0 used in the model arises from the constraint of equal variance of finestructure and internal waves found in the β-domain (Levine and Irish, 1981). In region II, we see strong evidence that the internal wave model is correct. The differing spectral forms of $\omega^{-1.5}$ for the moored spectrum and $\omega^{-2.5}$ for the travel time spectrum supports the effect of the internal wave dispersion relation (i.e. the travel time spectrum differs in spectral slope by -1 from the temperature spectrum). Also, the spectral cutoffs, the value of p, and the normalization of the model are supported. In region III, the ω^{-3} spectral slope of the moored spectrum and the ω^{-4} spectral slope of the travel time spectrum provides strong evidence that the high wavenumber finestructure is advected by internal waves (hence the effect of the internal wave dispersion relation).

We have attempted to show both the complexity of the ocean TCF as well as the large diversity of oceanographic data needed to confirm ocean spectral models. The ability of the acoustic field to give us an integral constraint on the model through phase correlations must be emphasized. It should also be emphasized that the inversion was done individually on each data set. A combined inversion is also possible (and is under proposed study). The combined inversion would impose, in a consistent manner, the relationships between the oceanographic and acoustic data sets exhibited in Figure 6. A future combined oceanographic/acoustic experiment would exploit these same relationships in a test of the new dynamical internal wave model.

AATE ACOUSTIC FIELD MEASUREMENTS

MATE demonstrated that the acoustic scattering conditions can be determined when extensive environmental measurements are made simultaneously with acoustic field measurements.

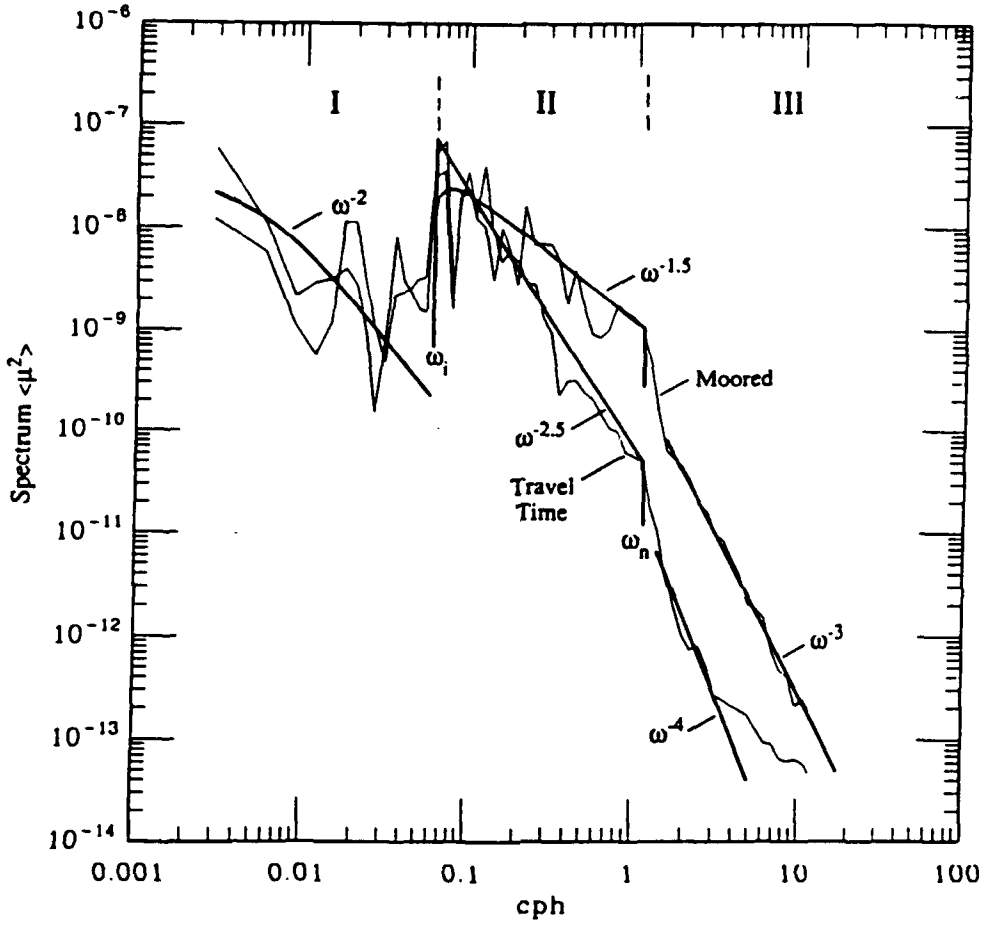

Figure 6. Plots of the travel time and moored temperature spectra in $<\mu^2>$ units. The tidal components have been removed; only the stochastic components remain in the data.

Although MATE provided a long series of temporal acoustic measurements, only a few spatially separated receivers were used. To augment our understanding of the spatial characteristics of the scattered field, AATE (the AIWEX Acoustic Transmission Experiment) was designed to make both vertical and temporal measurements of the acoustic field. The transmission experiment (conducted under multi-year ice in the central Beaufort Sea) consisted of four co-located transmitters (2,4,8,16 kHz) suspended beneath the ice at 153 m depth. These were positioned 6.43 km from a depth cycling array of 3 receivers, separated by 51 m (the depth cycle was 51 m providing a 153 m vertical aperture). Simultaneous environmental measurements were made by several investigators from several institutions. A study of AIWEX moored data by Levine (1990) has resulted in an internal wave model.

Figure 7 displays the travel time and log-intensity spectra measured over two time periods during AATE. (A strong wind event occurred between the two time periods, making interpretation of the travel time measurements across the event difficult, if not impossible.) The spectra in Figure 7 may be compared to those taken during MATE. Predictions from the weak-scattering theory of Desaubies (1978) are shown with the observations from before the wind event. The acoustic fluctuations are significantly less energetic ($\simeq$ 1/50th) than those expected under canonical GM, open ocean conditions (the GM-parameters have been adjusted for the AIWEX buoyancy frequency profile). In addition, the spectral slope of the travel time spectra is a power less than the prediction. These results are similar to those obtained from measurements made at the AIWEX environmental moorings (Levine, 1990). Note that the travel time spectra observed after the wind event display a peak at the local inertial frequency. This feature is also seen in the two dimensional 2 kHz travel time spectra shown in Figure 8. The presence of the inertial peak after the wind event shows a serious lack of stationarity. This complicates modeling, but also indicates that additional interesting oceanographic processes were present after the wind event. Sorting out the mechanisms requires close examination of the environmental data taken during these two time periods.

A goal was to invert the AATE acoustic phase measurements and obtain a prediction for the internal wave/finestructure spectrum, analogous to what was done with the MATE results. Though the AATE travel time measurements were made to accuracies of a few microseconds out of a total travel time of 4 seconds, the travel times are contaminated by mooring motions of less than 1 cm. This contamination makes their use for an inversion problematic. However, when the scattering is sufficiently weak, stochastic inverse predictions are possible from the amplitude measurements. Under the conditions of AATE, we should be able to obtain the environmental field from inversion of the log-amplitude statistics. This analysis remains to be completed. The value of the spatial inversion is implied by the predictions shown in Figure 9. These are the wavenumber spectral filters of acoustic phase and log-amplitude obtained from the Rytov predictions of Desaubies (1978). The predicted phase and log-amplitude spectra are obtained by multiplying the medium spectrum, $S(\beta,\omega)$, by the appropriate filter function.

Note that for more traditional open ocean scattering conditions, the acoustic intensity probably cannot be used as an inversion tool. It is beyond the scope of this paper to discuss comparisons between theory and measured intensity statistics. But for propagation ranges more than a few kilometers in most of the ocean, a multiple-scattering theory is required. When the field has been multiply scattered, the intensity statistics can no longer be understood as the action of a linear filter, like that shown in Figure 9. Fortunately though, the multiple scattering effect on the acoustic phase is small enough that it can be used as an inversion tool apparently even for long range cases. Although the AATE measurements provided measurements both in the vertical and in time, the weak acoustic phase fluctuations were masked by small mooring motions. Because virtually no other space/time measurements of the acoustic field have been made under conditions where the scattering field is known, further studies of the stochastic inverse methodology requires, at least for the near future, taking a numerical approach. Our current work presents some examples relevant to the oceanographic community and demonstrates the validity of this approach.

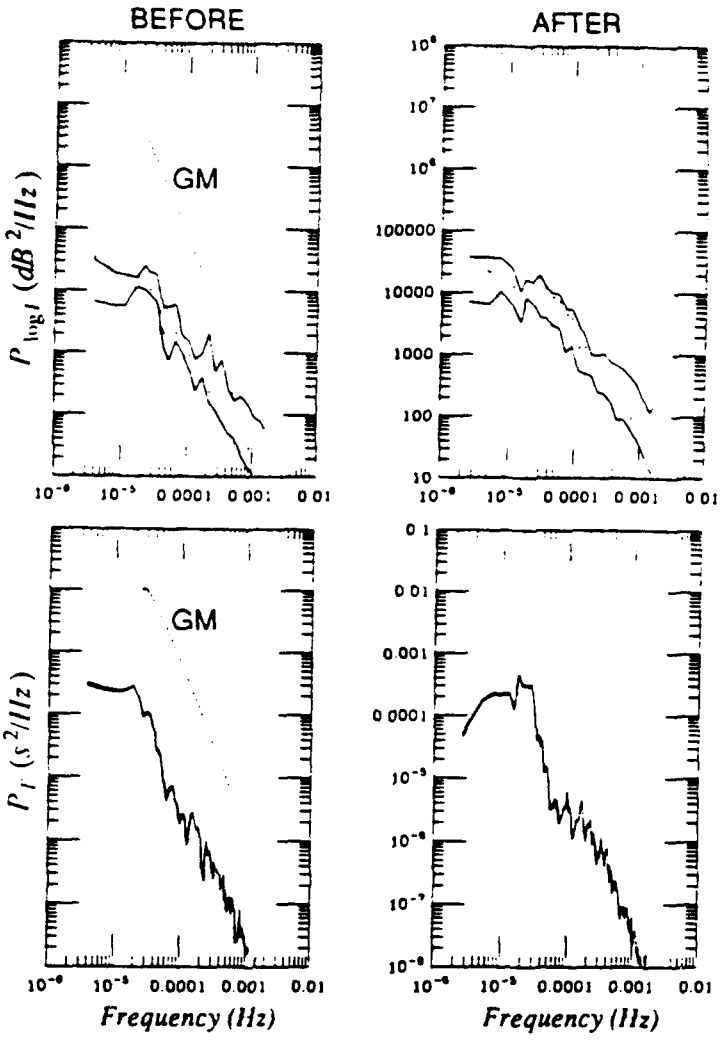

Figure 7. AATE observed log-intensity and travel time spectra for a 3 day time period before a wind event and a 4.3 day time period after the same event. To show the temporal behavior, a fixed depth data series was obtained. Spectra obtained from the 2, 4 (dashed) and 8 kHz data sets are shown. Predictions obtained using the canonical GM-model are overplotted on the left-hand graphs.

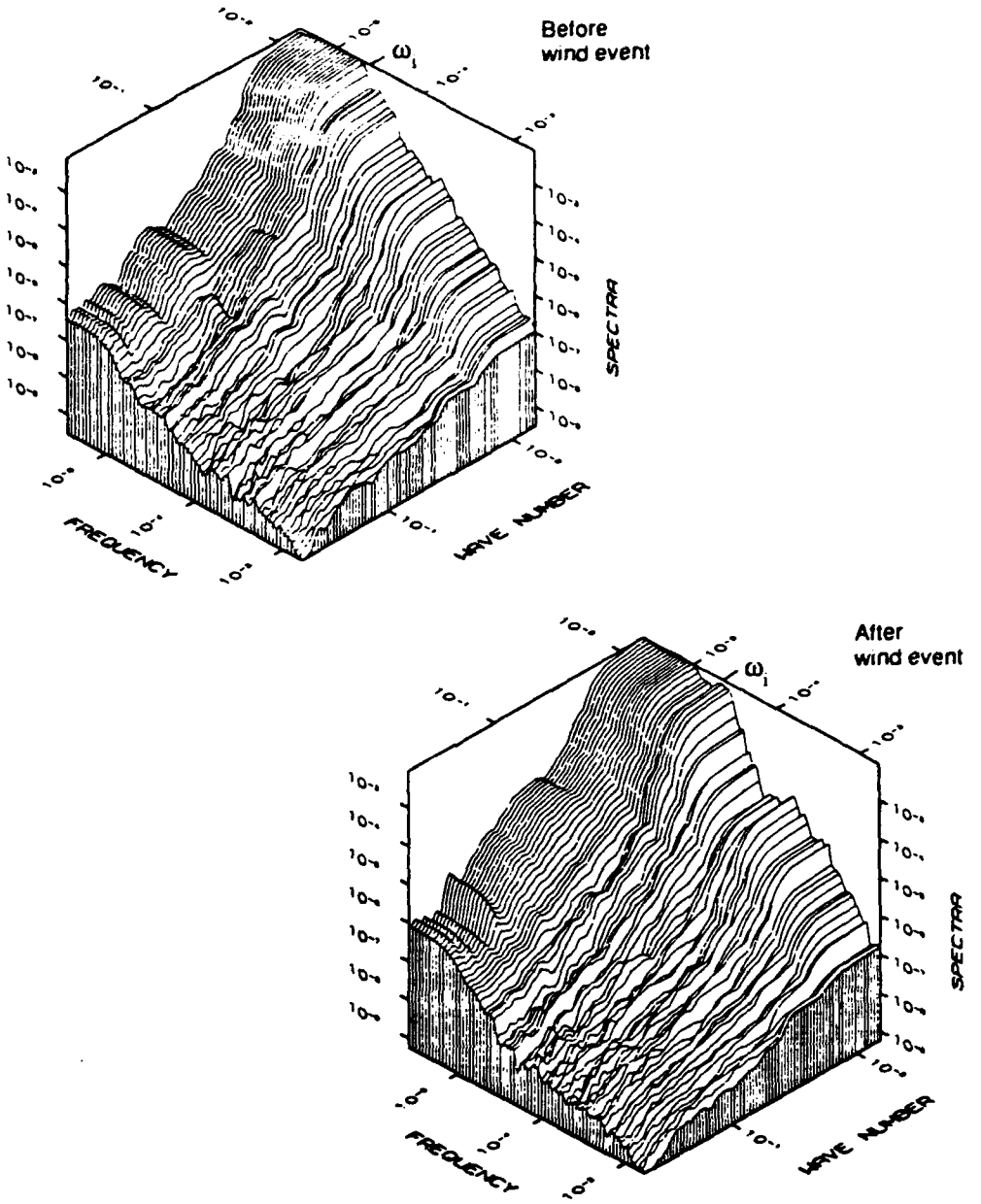

Figure 8. AATE travel time spectrum as a function of vertical wavenumber and frequency estimated from the 2 kHz measurements. A peak is observed near the inertial frequency in the spectrum from after the wind event.

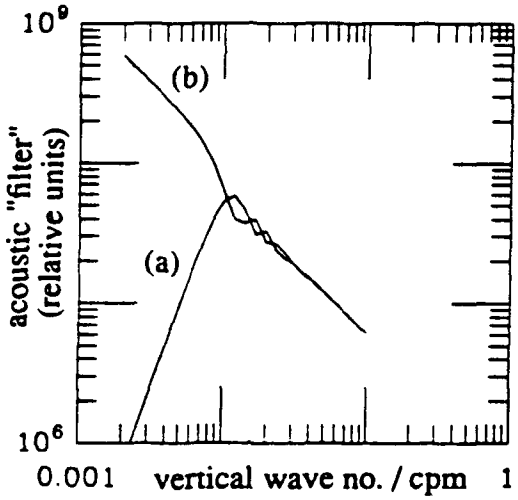

Figure 9. The acoustic filters as functions of vertical wavenumber for $\omega = .3$ cph that act on the medium spectrum for the log-amplitude (a) and phase (b). These functions were obtained using the weak-scattering theory of Desaubies (1978).

NUMERICAL SIMULATIONS AND THEORY

Much has been learned about acoustic fluctuations from numerical simulations. An example is its use in testing acoustic scattering theory. The technique of using parabolic equation propagation codes to test moment theoretical predictions was initiated by Macaskill and Ewart (1984). Since then, their technique has been modified to include a point source initial condition and other important physics. The moment theories are full range theories, and not asymptotic at short or long range; thus, they are important to ocean acoustics.

Figure 10 shows a contour plot of the normalized intensity variance (traditionally called the scintillation index) as a function of acoustic frequency and range (from Ewart, 1989). The input ocean model used for the TCF is $R_{\perp}(\zeta) = (1 + |\zeta|/L_v)\exp(-|\zeta|/L_v)$ which is asymptotically β^{-4} in the vertical wavenumber domain. The normalization is typical of mid-ocean internal waves with $<\mu^2> = 3.0 \cdot 10^{-9}$, $L_p = 4600$ m, and $L_v = 150$ m. For frequencies above 1 kHz, the scintillation index rises to a maximum at a location called the focus of the medium, and then decays to a value of one. The noise cutoff, plotted as a heavy solid line, demonstrates that for frequencies above 1 kHz, reaching long ranges will be difficult in the ocean.

For our purposes, it is important to note that Uscinski's full range theory for plane wave propagation is in excellent agreement with the plotted scintillation indices, and with the vertical wavenumber decomposition of the intensity variance. Similar studies of the point source initial condition display a scintillation peak that is higher. These features are also obtained with theory. Uscinski (1989) has demonstrated that when using parabolic equation propagation in polar coordinates (the natural coordinates for a point source) the predictions from moment theory and results of the simulations agree to within statistics. For that work a Gaussian TCF was used, and more work remains to be done for power law media such as the case with internal waves. But the overall agreement demonstrates that the moment theory solutions are robust over diverse scattering conditions and ranges. The underlying point is that, for a given medium transverse correlation function, the numerical experiments have shown that available theories of stochastic wave propagation can predict the second and fourth moments of the acoustic field. Our ability to predict acoustic fluctuation statistics under true ocean conditions then depends upon the validity of the TCF, and hence the importance to acoustics of the new internal wave modeling effort.

WHAT SCALES ARE IMPORTANT FOR ACOUSTICS?

Our last example is from numerical evaluation of theory. The example comes from asking the question, "If an oceanographer made vertical measurements of sound speed fluctuations, what scales in those measurements are important in predicting acoustic volume scattering?". This question has been addressed in recent work by Ewart and Ballard (1990). They attempted to establish the small scale limit for oceanographic measurements required to predict the scintillation index, given a known TCF. Because ocean scattering is characterized by weak but multiple scattering, all scales of the medium can theoretically contribute to all scales in the prediction of the acoustic intensity. Using Uscinski's theory to predict the intensity fluctuations with depth, the following computation was carried out. Using a TCF derived from the internal wave model presented in Levine and Irish (1981), and a specific range and scattering strength, a prediction for the scintillation index was obtained for the condition of an inner scale wavenumber cut-off in the transverse spectrum of 0.1 cpm (10m). Denote this value of the scintillation index

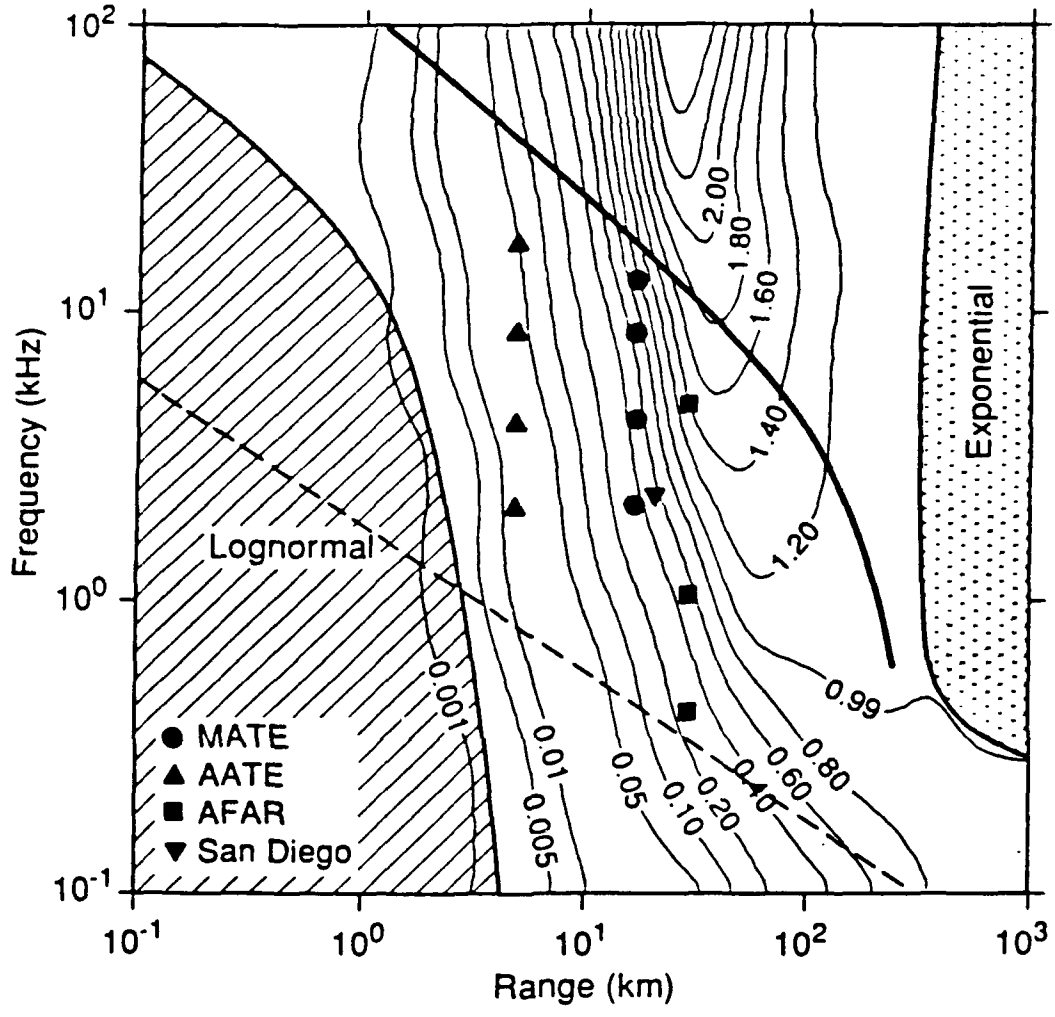

Figure 10. Contours of the normalized intensity variance vs frequency and range. Crosshatched areas are the asymptotic regions for the log-normal and exponential distributions. The solid line shows the range limit for a 200 dB source (for Sea State IV noise levels), and the dashed line is the boundary for multiple scattering.

as SI_t. The cut-off wavenumber was then decreased until a scintillation index equal to .9 or 1.1 of SI_t was reached. The two regions correspond to before and after the medium focus. This process was then repeated for a wide range of scattering strengths and ranges. A contour plot of these 90% and 110% cut-off wavenumbers as functions of acoustic frequency and range is shown in Figure 11. (This parameterization requires selecting specific internal wave model parameters, the ones listed above were used.) The bold line shown corresponds to the noise limit for a 200 dBμPa/m source; the light solid line denotes the multiple scattering boundary. The result is that for ranges greater than a few kilometers and frequencies less than 10 kHz, small vertical scales contribute little to the scintillation index. Note also that the smaller scales become less important as the range (and hence cumulative scattering) increases.

In the numerical simulations, the medium is treated as consisting of δ-correlated phase changing screens that are statistically described by the TCF. The question, "Is it theoretically permissible to represent the ocean statistics in this manner?" has been studied in additional research conducted by Ewart and Kaczkowski (1990). They have studied medium models that are correlated in range, versus those described by δ-correlated screens (i.e. a Markov process). Their research shows that little difference exists in the acoustic field moments for the two descriptions. This result, when considered with the observations presented in the previous paragraph on the effects of changing the inner scale, allows us to simplify oceanographic modeling for simulating acoustics. This simplification is incorporated into our discussion of dynamical modeling in the Summary section.

SUMMARY AND WHAT'S NEXT?

We have provided a brief tutorial on the connectivity between ocean stochastic modeling and predictions of the moments of an acoustic wave propagating through such an ocean. In this section we include a brief summary of our main points and mention desirable future directions for research.

Summary

- Internal wave models (new and used), are vital for predicting the statistics of acoustic propagation.
- Stochastic inverse methodology provides a tight check on proposed new models, when sufficiently careful space/time acoustic observations are made simultaneously with space/time oceanographic observations. The use of both oceanographic and acoustic measurements in combination must be emphasized.
- The missing element in research is the availability of acoustic observations in depth/time, where the medium correlation function is known.
- Numerical experiments, where dynamical models are used to define the index of refraction field, may help us to understand stochastic inverse methods, **BUT,**
- Field experiments with sufficient space/time measurement bandwidth must be coupled with acoustic measurements ----
    - We must measure the complex acoustic field $E(z,t)$ for several frequencies and ranges.
    - When a "new model" is available, a detailed experiment can be designed with numerical modeling.

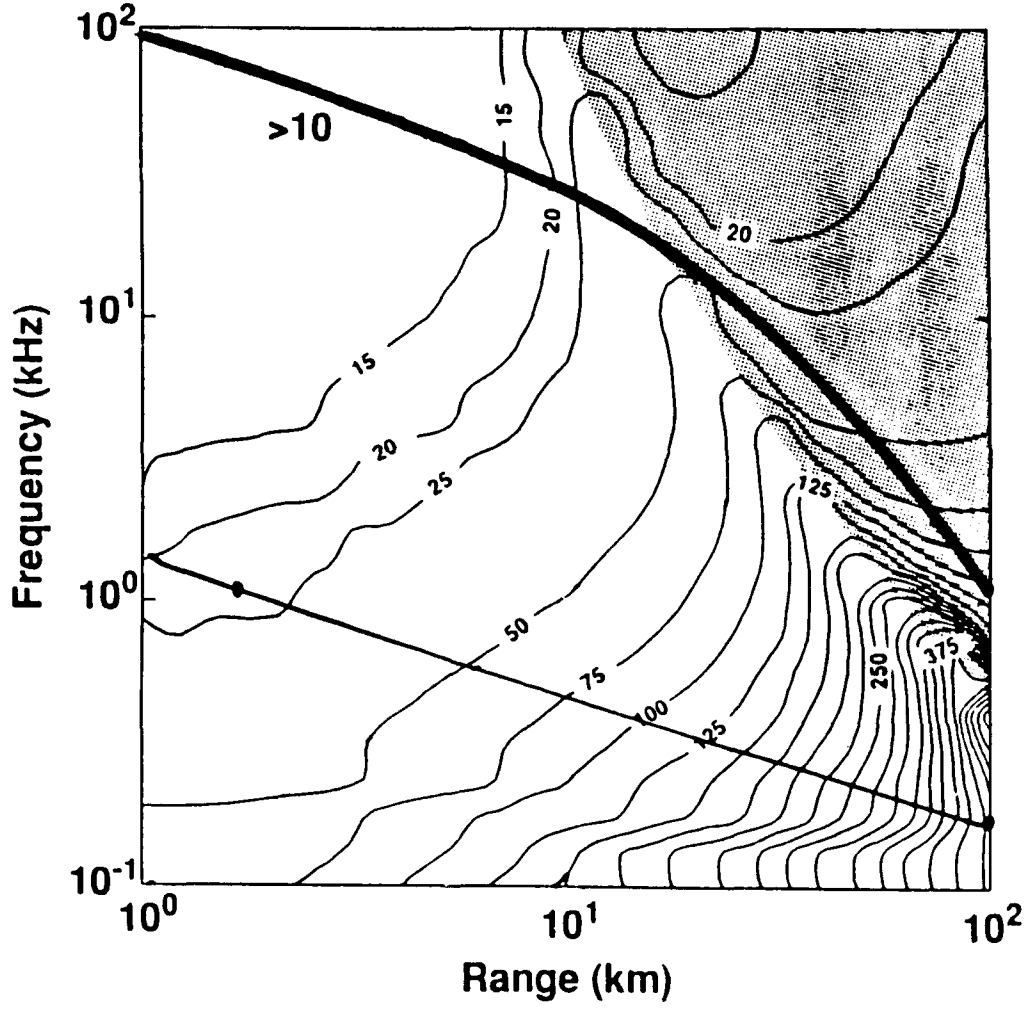

Figure 11. The vertical scale to reach 90 or 110 % of the scintillation index calculated to a limit of 10 m (see text) as a function of range and acoustic frequency. The contours are derived by selecting the MATE values of $\langle\mu^2\rangle^{1/4}$, L_p and L_v. As in Figure 10, the bold line corresponds to the noise limit for a 200 dBμPa/m source, the thin line denotes the multiple scattering boundary. In the region denoted ">10", the cutoff is at the Levine/Irish inner scale, and hence unchanging.

3-D Dynamical Modeling

We have stated emphatically that the lack of high quality data prevents us from testing the stochastic inverse methodology on the range of space/time scales that are relevant to the modeling goals of the 'Aha Huliko'a meeting. Using the insight we have gained from studying modeling limits, we are collaborating with Kraig Winters and Eric D'Asaro (See their contributions in this proceedings) to test the capabilities we have developed in theoretical predictions and stochastic inverse methodology with their dynamic simulation modeling. The proposed model, to be run on our Stardent Mini-Supercomputer, will have horizontal scales of 50 by 20 km in x and y respectively (x is the propagation direction) and 2000 m in the vertical. Its corresponding resolution will be 20 m in the vertical and 333 m in the horizontal with a grid of $128^3/4$ cells. The model will be initialized in several ways and run with time steps spanning many inertial periods. The resulting density fields will be the input to our PE propagation codes and will provide simulated realizations of the acoustic field. This type of modeling is very important, because it allows us to demonstrate the necessity (or lack thereof) of including dynamics in acoustic modeling.

Realizations of 3-D plus time density fields can also be produced from any proposed model, and used via Monte Carlo methods to test the stochastic inverse concepts discussed here. In verifying acoustic scattering predictions, one can test the robustness of the predictions to relaxed assumptions in the model, e.g., fully random phase versus dynamically consistent, and correlated versus Markov medium representations. All of these issues are relevant to our computer-limited ability to model acoustic propagation.

A Proposed Experiment

Eric D'Asaro has proposed an internal wave experiment designed to test many of the existing ideas on the cascade of energy from low internal wave modes to higher modes. The experiment would be conducted far from boundaries and sources of low mode internal wave energy. For example an area south of a storm region could be used to study how a changing flux of low mode internal wave energy "pumps" a local internal wave space/time spectrum. An extensive suite of dynamic and scalar oceanographic measurements would be made over a long period of time in order to develop an understanding of the linear and nonlinear processes involved. We would propose that an acoustics experiment capable of measuring the complex field at many spatially separated points be made an integral part of the overall measurement program. Many of the ideas we have presented here could be implemented. By sensing such a large volume of the experimental region, the acoustic measurements we envision would provide a severe constraint on possible space/time models.

ACKNOWLEDGEMENTS

The authors would like to thank Dr. John Ballard for carrying out the evaluations of theory. Nina Triffleman edited our efforts and produced it in camera ready finished form. This research was sponsored by the Department of the Navy, Office of the Chief of Naval Research, under Grant N00014-90-J-1260. This article does not necessarily reflect the position or the policy of the Government, and no official endorsement should be inferred.

REFERENCES

Desaubies, Y.J.F., 1976, Analytical representation of internal wave spectra, *J. Phys. Ocean.*, 6(6), 976-981.

Desaubies, Y.J.F., 1978, On the scattering of sound by internal waves in the ocean, *J. Acoust. Soc. Am.*, 64(5), 1460-1469.

Ewart, T.E., 1986, Acoustic propagation, internal waves, and finestructure, *Proc. Instit. Acoust.*, 8 (Part 5), 106-122.

Ewart, T.E., 1989, A model of the intensity probability distribution for wave propagation in random media, *J. Acoust. Soc. Am.*, 86(4), 1490-1498.

Ewart, T.E. and J. Ballard, 1990, Coupled volume and surface scattering, *J. Acoust. Soc. Am.*, Suppl. 1, 88, S44.

Ewart, T.E. and P. Kaczkowski, 1990, Simulating stochastic scattering in ocean acoustics: How complex a model do we need ?, 1990 (unpublished manuscript).

Ewart, T.E., C. Macaskill and B.J. Uscinski, 1983, Intensity fluctuations. Part II: Comparison with the Cobb experiment, *J. Acoust. Soc. Am.*, 74(5), 1484-1499.

Ewart, T.E. and S.A. Reynolds, 1984, The mid-ocean acoustic transmission experiment, MATE, *J. Acoust. Soc. Am.*, 75(3), 785-802.

Levine, M.D., 1990, Internal waves under the Arctic ice pack during AIWEX: The coherence structure, *J. Geophys. Res.*, 95(C5), 7347-7357.

Levine, M.D. and J.D. Irish, 1981, A statistical description of temperature finestructure in the presence of internal waves, *J. Phys. Ocean.*, 11(5), 676-691.

Levine, M.D., J.D. Irish, T.E. Ewart and S.A. Reynolds, 1986, Simultaneous spatial and temporal measurements of the internal wave field during MATE, *J. Geophys. Res.*, 91(C8),9709-9719.

Macaskill, C. and T.E. Ewart, 1984, Computer simulation of two-dimensional random wave propagation, *I.M.A. J. Appl. Math.*, 33, 1-15.

Munk, W., 1981, Internal waves and small-scale processes, in *Evolution of Physical Oceanography*, edited by B. A. Warren and C. Wunsch, MIT Press, 264-291.

Slepian, D., 1978, Prolate-spheroidal wave functions, Fourier analysis and uncertainty - V: the discrete case, *Bell Syst. Tech. J.*, 75(5), 1371-1430.

Uscinski, B.J., 1980, Parabolic moment equations and acoustic propagation through internal waves, *Proc. R. Soc. Lond.*, A(372), 117-148.

Uscinski, B.J., 1986, Acoustic scattering by ocean irregularities: Aspects of the inverse problem, *J. Acoust. Soc. Am.*, 79(2), 347-356.

Uscinski, B.J., 1989, Numerical simulations and moments of the field from a point source in a random medium, *J. Mod. Optics*, 36(12), 1631-1643.

Uscinski, B.J. and J.R. Potter, 1988, Sound ribbons in the Sea, *Acoustics Bulletin*, Oct.